Atmos. Chem. Phys. Discuss., 10, 13495–13517, 2010
www.atmos-chem-phys-discuss.net/10/13495/2010/
doi:10.5194/acpd-10-13495-2010

Atmospheric Chemistry and Physics Discussions

Mesoscale processes for super heavy rainfall of Typhoon Morakot (2009) over Southern Taiwan

C.-Y. Lin[1], H.-m. Hsu[2], Y.-F. Sheng[1], C.-H. Kuo[3], and Y.-A. Liou[4]

[1]Research Center for Environmental Changes, Academia Sinica, Taipei, Taiwan
[2]National Center for Atmospheric Research, Boulder, Colorado, USA
[3]Department of Geology, Chinese Culture University, Taiwan
[4]Center for Space and Remote Sensing Research, National Central University, Taiwan

Received: 20 April 2010 – Accepted: 20 May 2010 – Published: 27 May 2010

Correspondence to: C.-Y. Lin (yao435@rcec.sinica.edu.tw)

Published by Copernicus Publications on behalf of the European Geosciences Union.

Abstract

Within 100 h, a record-breaking rainfall, 2855 mm, was brought to Taiwan by Typhoon Morakot in August, 2009 resulting in devastating landslides and casualties. Analyses and simulations show that under favorable large-scale situations, this unprecedented precipitation was caused first by the convergence of the southerly component of the pre-existing strong southwesterly monsoonal flow and the northerly component of the typhoon circulation. Then the westerly component of southwesterly flow pushed the highly moist air eastward against the Central Mountain Range, and forced it to lift in the preferred area. The mesoscale processes in two stages were responsible for the unprecedented heavy rainfall total that accompanied this typhoon. Thus, understanding the dynamical interactions between the typhoon's circulation and monsoonal flow at different scales should enhance the forecasting capability in precipitation events brought by similar typhoons in the future.

1 Introduction

2885 mm (112.4 inches) rainfall in 100 h, much more than the mean annual precipitation, was recorded at A-Li Shan Mountain station (23.5° N and 120.8° E, 2413 m in elevation) as Typhoon Morakot (2009) traversed the island of Taiwan during the 5-day period (6–10 August 2009). It was the heaviest total rainfall for a single typhoon impinging upon the island ever. This typhoon has set many new records in Taiwan. Nine of the ten highest daily rainfall accumulations in the historical record were made by Typhoon Morakot, according to the Central Weather Bureau (CWB). Among them, Wei-Liou San station (elevation about 710 m in southern Taiwan; 22.82° N and 120.66° E) recorded as high as 1403 mm rainfall in one day, 8 August. Table 1 provides a list of the 10 highest rainfall accumulations by typhoons during the last 50 years in which two types of typhoon passages were characterized. One traverses the Central Mountain Range (CMR), the primary island mountain, in the summer (June to August), and the other

ACPD
10, 13495–13517, 2010

one passes nearby the island with northeasterly monsoon flow in the fall (September to November). This is the first typhoon simultaneously accompanied with strong southwesterly monsoon and it generates 2 to 3 times more mean daily rainfall than the nine other strongest typhoons during the last 50 years (Table 1). Typhoon Morakot also was responsible for a vast area, over the western hilly regions of the Central Mountain Range, receiving more that the one year average precipitation(2000 mm) in just 3 days (7–9 August) (Fig. 1d). This unprecedented rainfall accumulation and area covered are bound to cause disasters.

In just three days, there were enormous landslides triggered in mountainous terrains and severe flooding blanketed large areas of lowlands. One particular landslide occurred in the early morning on 9 August, burying the entire village of Xiaolin (elevation around 345 m located at valley, 120.65° E and 23.17° N, in Kaohsing county in southern Taiwan), killing more than 600 people in this village alone (Fig. 2). In Fig. 2a, the effect of the landside is evident in the aerial photo of the region before the landslide (left) and after the landslide (right). The area damaged by the landslides, estimated by satellite FORMOSAT-2 (http://www.satimagingcorp.com/satellite-sensors/formosat-2.html), was 241.7 acres. The village of Xiaolin with nearly 394 houses and the nearby woodland were covered by mud completely (Fig. 2b). Roughly NT $ 16.4 billion (~US $ 0.5 billion) in agricultural damages alone has been estimated over Taiwan because of this tragic event. The official estimation of all the damages and reconstruction costs is beyond NT $ 100 billion (~US $ 3.03 billion).

As typhoons pass over the island of Taiwan and its vicinity, the local rainfall is strongly affected by the island mountains, particularly the Central Mountain Range (CMR). The CMR occupies about two-thirds of Taiwan's land mass (300 km × 100 km), and is oriented approximately N-S (Fig. 1b) with an average terrain height of about 2000 m (Chen and Li, 1995; Lin and Chen, 2002) and a few steep peaks of almost 4 km. It is well known that damages are strongly related to the location of the typhoon's landfall and interactions between its circulations and the CMR (Brand and Blelloch, 1974; Wu and Kurihara, 1996; Wu and Kuo, 1999; Lin et al., 2001; Chien et al., 2008; Ge et al.,

ACPD
10, 13495–13517, 2010

2010). Previous studies pointed out that enormous amounts of rainfall occur and are enhanced due to mountain lifting when a typhoon passed over the CMR (Wu and Kuo, 1999; Lin et al., 2002). In addition, the CMR is crucial and plays an important role in modifying the rainfall distribution (Wu et al., 2002; Wu and Kuo 1999; Lin et al., 2001; Yang et al., 2008). Moreover, it is common that the strong southwesterly flow follows the departure of an invading typhoon and brings heavy rainfall over central or southern Taiwan (Lee et al., 2008; Chien et al., 2008). Sometimes, such rainfall associated with the southwesterly flow can even be significantly heavier than the rainfall brought by the typhoon itself (Chien et al., 2008).

The large-scale settings for the track and intensity of any tropical cyclone are important, but the primary cause for the extreme rainfall may vary. Ge et al. (2010) suggested the critical role of the CMR and the large-scale conditions for Morakot in their numerical experiments at 3-km resolution. Their control case resulted in a maximum rainfall total of more than 1800 mm. All of their conditions are necessary for Morakot's circulation and evolution, but insufficient for this unprecedented rainfall of the 2885-mm maximum. Here, not only do we apply the same numerical model (ARW) with a coarser resolution (10 km) to simulate the total rainfall (2348 mm maximum) more closer to the observed than that of Ge et al. (2010) without any special initialization procedure, but also identify the most important and direct dynamic process for the unprecedented downpour over the southern Taiwan. The process is that this unprecedented precipitation was caused first by the convergence of the southerly component of the pre-existing southwesterly flow and the northerly component of the typhoon circulation. Then the westerly component of southwesterly flow from the South China Sea joined the system to push the highly moist air eastward against the CMR, and forced it to lift in the preferred area. The coexistence of both processes was responsible for the unprecedented heavy rainfall. In fact, this combination of processes can be revealed by analyzing the large-scale meteorological analysis data in conjunction with the station data.

ACPD
10, 13495–13517, 2010

Title Page
Abstract | Introduction
Conclusions | References
Tables | Figures
◂◂ | ▸▸
◂ | ▸
Back | Close
Full Screen / Esc
Printer-friendly Version
Interactive Discussion

2 Data sources and model description

We analyzed the rainfall data from CWB rainfall stations (Fig. 1b; red dots, 426 stations in total) monitoring network as well as the archived radar and satellite data of CWB. The moisture flux and air flows were deduced from the National Centers for Environmental Predictions (NCEP) Global Forecast System (GFS) $0.5^{\circ}\times0.5^{\circ}$ analysis data sets (26 vertical levels) at 6-h interval.

The Advanced Research WRF (Weather Research and Forecast) model has been configured for the numerical experiments of Morakot. In order to provide detailed and dynamic consistent information of this typhoon, the results of rainfall from one particular simulation are assessed by the CWB raingauge measurements and further illustrate the usefulness of numerical models. The details of the Advanced Research WRF (ARW) can be found in Skamarock et al. (2008). The initial and boundary conditions for ARW simulation are also interpolated from NCEP/GFS data sets. In this simulation, the Yonsei-University and the WRF Single-Moment 5-class schemes were selected for the planetary-boundary-layer and microphysics parameterizations, respectively. There were 45 vertical levels and the lowest level was about 50 m above the surface. The horizontal resolution was uniformly 10 km in both directions, with 1081×691 grid-points. Cumulus parameterization may not be necessary at this resolution (Knutson et al., 2007). Thus, no cumulus parameterization was activated in the simulation presented here. To ensure that this event was well simulated, the four-dimensional data assimilation scheme was activated based on the NCEP-GFS analysis data.

3 Data analysis

3.1 Typhoon track and rainfall

Figure 1a shows the best track of Morakot and indicates the typhoon began as a tropical depression near 135° E, 20° N on 4 August and continuously moved westward. After upgrading to an intermediate typhoon (Fig. 1a) with maximum wind speed at nearly 40 m/s during 5 August, it approached Taiwan on 6 August. Since Morakot made landfall at 18:00 UTC 7 August, it quickly downgraded to a light typhoon (maximum wind speed was less than 32.6 m/s). Its structure became incoherent and a distinctive eye did not seem to exist. Instead, the storm had a very asymmetric structure with a broad rainband 150–300 km wide, east of center, with radius of curvature 250 km covering the entire Taiwan (Fig. 3a–c), as it moved slowly after 7 August (Fig. 1a).

After averaging the measured rainfall data between 120 and 121° E (bounding horizontally the black dashed square in Fig. 1b), the rainfall evolution spanning this square from south to north is displayed for a period of 9 days (Fig. 1c). The rainfall over the western slopes of the CMR lasted for at least 4 days (12:00 UTC 2 August ~ 12:00 UTC 6 August) before Morakot impinged upon Taiwan. The 24-h rainfall totals in these first 4 days limited to 150 mm, were supported by the moist southwesterly flow in the lower troposphere. In fact, this southwesterly flow had come from South China Sea since 2 August and continued to prevail since (Fig. 4b and c).

The latitudinal extent is divided into three regions from northern to southern Taiwan, named N, C, and S, which ranges from 24.0 to 25.0° N, from 23.0 to 24.0° N and the extent south of 23.0° N, respectively (Fig. 1c). Only weak rainfall occurred over mountainous areas during 3–5 August before the typhoon affected Taiwan. Significant precipitation began over the area near 22° N after 7 August, especially around 00:00 UTC 8 August, and then gradually moved northward through the region C between 22.4° N and 23.6° N, ending about 06:00 UTC 9 August. After it made landfall on the eastern coast of Taiwan, Morakot weakened and lost its eye-wall structure as shown by radar and satellite images (Fig. 3a and b). On the western side of the CMR, the lower-tropospheric wind was dominated by northerly over the northern half while southwesterly over the southern half. Subsequently, precipitation began to increase significantly over the region S from 12:00 UTC 6 August and became torrential on the hilly areas after 12:00 UTC 7 August for about 24 h (Fig. 1c). During this period, more than 1000 mm was pouring in a narrow N-S belt (about 50×25 km^2) over mountain-

ACPD
10, 13495–13517, 2010

ous area. As described earlier, the tragic landslide occurred in the early morning of 9 August and buried the entire village of Xiaolin. Morakot made landfall again after 12:00 UTC 9 August on the southeast coast of China. However, as much as 350 mm additional rainfall accumulation took place during the following 24 h (i.e. on 10 August) over the already seriously damaged areas of southern Taiwan owing to the rainfall generated by the following southwesterly flow with its high moisture content (Fig. 3e).

3.2 Sources of the water vapor

After the horizontal moisture fluxes in the lower troposphere were computed using the NCEP/GFS analysis data, they were vertically averaged below 700 hPa (about 3 km) and zonally averaged between 119 and 121° E (the red square in Fig. 1a). Figure 4 shows the temporal evolutions of the zonal mean for vector moisture flux ($q \cdot U \hat{i} + q \cdot V \hat{j}$, where q = specific humidity), the zonal flux component ($q \cdot U$), and meridional component ($q \cdot V$) from 2 to 11 August over a latitudinal extent between 21 and 26° N. The contour lines denote wind speeds, while color shades represent the magnitude of the moisture fluxes.

The moisture flux shown in Figs. 3c–d and 4a displays a classical pattern of a tropical cyclone traversing the island. The moisture transport was mostly southerly before the arrival of Morakot. The passing of Morakot brought in a large amount of moisture in a cyclonic pattern around 7 August, mostly in southern Taiwan. After Morakot left the region (the red square in Fig. 1a) during 10 August, the moisture flux decreased to an overall southwesterly pattern.

Furthermore, for the E-W component (Fig. 4b), along 22.5° N (and farther south), the moisture flux >200 g/kg m/s (colored) started from 12:00 UTC 6 August and significantly increased to >500 g/kg m/s from 12:00 UTC 7 August to 12:00 UTC 8 August. The enormous moisture flux, >500 g/kg m/s, with strong westerly wind, >20 m/s (solid line in Fig. 4b), moved from the ocean toward inland including the mountainous areas and extended northeastward to 23° N around 00:00 UTC 8 August (Fig. 4b). This

ACPD
10, 13495–13517, 2010

is consistent with the torrential rains recorded in region S at the same time (Fig. 1c) and also agrees with the spatial distribution of extreme rainfall accumulation amount from the coastal plain area to CMR (Fig. 1d). In the evolution of the N-S component of the moisture flux from 2 August to 11 August (Fig. 4c), the southerly high moisture flux (>200 g/kg m/s) with wind speed >10 m/s already existed prior to 3 August before Morakot approached Taiwan. In other words, the southwesterlies with high moisture content prevailed during early August and lasted to 11 August at least in the lower troposphere (Fig. 4b and c). The strong southerly component of the moisture flux provided the source for the rainfall throughout this period, except for the invasion of the northerly flow of Morakot for a period between 6 August and 8 August. The northerly moisture flux with a wind speed >20 m/s (dashed line) associated with the typhoon invasion enhanced the north-south convergence (Fig. 4c). Consequently the moist southerly flux advanced northward, strengthened and collided with the northerly flux to form a local moisture convergence between 22 and 23° N during 7 August. This essential convergence of these two opposite fluxes hence played a key role in the dramatic increase of the rainfall (Fig. 1c) over southern Taiwan between 00:00 UTC 7 August and 00:00 UTC 8 August.

As Morakot slowly departed from the island and the associated northerly flux shifted northward, both the E-W convergence zone and the westerly moisture flux gradually traversed northward altogether. Eventually, the northerly flux was completely replaced by the southerly flux over the entire Taiwan after 00:00 UTC 9 August (Fig. 4a). However, some precipitation continued as a southerly moisture flux still prevailed. This fits the commonly recognized understanding that the southwesterly flow follows the departure of tropical cyclones from Taiwan.

It is well known that the southwesterly moist flow can contribute localized rainfall, but cannot alone support extreme amounts. The northerly flow of the Morakot's circulation collided with the southerly component of the southwesterly monsoon and produced a low-level convergence. This convergence became a critical factor in this significant rainfall occurrence over southern Taiwan during the early stage of heavy rainfall, which

ACPD
10, 13495–13517, 2010

Mesoscale processes for super heavy rainfall of Typhoon Morakot

C.-Y. Lin et al.

is illustrated in the following.

3.3 Depth of moisture flux

Figure 4d and e shows three-dimensional views in different perspectives for the moisture flux from the southwest (green arrow) at 00:00 UTC 8 August deduced from NCEP data by using VIS5D software (http://www.ssec.wisc.edu/~billh/vis5d.html). Comparing with the Morakot moisture-flux layer further northeast, the depth of moisture flux provides a better view of the entire process and the moisture layer from the southwest is really shallow, as seen in the northwest-southeast vertical perspective view (Fig. 4d). The more horizontal view (Fig. 4e) than the vertical one further illustrates that the southwesterly moisture flux was limited to a much lower altitude, below 900 hPa from the ocean surface at the southern end. This demonstrates the southwesterly flow has the capability to provide abundant moisture even though shallow, below 900 hPa from the ocean surface at the southern end.

Moreover, Fig. 4e illustrates that the moisture flux gradually thickened toward Morakot's layer in the north. The red, southwesterly, and light-blue, westerly flows, arrows denote the wind fields at 925 hPa and 650 hPa, respectively. It is apparent that the process of convergence started at the lower left corner of Fig. 4e and the lower altitude southwesterly flow did not reach the 900 hPa-level as it went into the moisture band. It also shows that the lower altitude southwesterly flow merged into the typhoon circulation and extended much higher than this level in the north. The co-existence of the tropical southwesterly moist flow in the low atmosphere and the relatively higher Morakot circulation is the key reason for the heavy rain production and wide-spread floods over southern Taiwan.

3.4 Horizontal convergence

To better understand the evolution of the convergence itself, we directly averaged the E-W and N-S components of the horizontal convergence derived from the NCEP/GFS

ACPD
10, 13495–13517, 2010

analysis between 120 and 121° E, which included the most western plain and hilly regions of Taiwan. Then they were averaged vertically between 950 and 700 hPa to represent the lower-tropospheric convergence. The N-S convergence (Fig. 5c) supported the heavy rainfall (Fig. 1c) during 7 August and early 8 August for the region south of 23° N. As heavy rainfall slowly moved northward after early 8 August, the E-W convergence took over. This shift diminished neither the intensity nor total rainfall, despite the E-W convergence (Fig. 5a) being weaker than its N-S counterpart. While the E-W convergence strengthened its N-S counterpart became divergence. The two convergence components evidently represent different processes. Figure 4d shows the gradually increase of moisture flux toward inland. And this E-W convergence in the region 23 ∼24° N continued to support heavy rainfall for at least 3 days along the western hills and slope of CMR (Fig. 1c). The NCEP/GFS analysis data have a horizontal resolution of about 50 km, which is too coarse to closely represent the convergence intensity. Thus results from a numerical experiment with higher resolution using ARW is presented next.

4 Model simulation

The numerical simulation was conducted with a version of the Weather Research and Forecast (WRF) model, the Advanced Research WRF (ARW3.1), for 4 days between 00:00 UTC 6 and 00:00 UTC 10 August. The 96-h simulation accumulation rainfall (Fig. 1e) matched the observations (Fig. 1d) quite well in terms of the rainfall amount (2348 mm) and spatial distribution. The underestimation of the rainfall accumulation by Ge et al. (2010) might be due to the resolution in the vertical and initial condition as well. The vertical levels are 27 in Ge et al. (2010) while 45 in our study. And the resolution of initial data may also attribute to this issue. The initial data used in our simulation is from NCEP GFS with 0.5° resolutions while Ge's study took from NCEP FNL data sets with 1°. We further plotted the time series of the E-W and N-S components of averaged convergence (Fig. 5b and d) as we did from the NCEP/GFS

ACPD
10, 13495–13517, 2010

analysis (Fig. 5a and c). Overall, the evolutions from the simulation are comparable to those from the analysis. One striking difference in the N-S components of the mean convergence is that the model evolution (Fig. 5d) is much stronger than that of the analysis (Fig. 5c), because of the difference in resolution. This convergence was the primary reason for the heavy rain in the S region (south of 23° N), as seen in Fig. 1c. Moreover, the E-W component of the convergence from the ARW simulation (Fig. 5b) was much stronger than that from the NCEP/GFS analysis (Fig. 5a), particularly for the latitudinal band between 23° N and 24° N. The dramatic enhancement by using 10 km resolution (Fig. 5b) was obvious. This enhancement of the convergence from model result indicates the significance of topographic lifting for producing the heavy rain during 8–9 August when the N-S convergence was relatively weakened. We are currently analyzing results from numerical experiments with finer resolutions.

5 Summary

Under the large-scale circulation of persistent southwesterly monsoon and the presence of CMR, unprecedented rainfall associated with Morakot caused tremendous damage over southern Taiwan. The mesoscale sequence can be described as follows. Based on our investigation of analysis data and model results, the first stage of the heavy rainfall during 7 and early 8 August was dominated by the N-S convergence south of 23° N in the low troposphere, and the second stage during the rest of 8 August was controlled by the E-W convergences and mountain blocking between 22.5 and 24° N. It is apparent that ARW with high enough resolution is able to simulate extreme rainfall well with the enhanced convergence comparing with that of NCEP/GFS data. The multi-scale nature of tropical cyclones for generating localized heavy rainfall requires further studies utilizing the available observational instruments and numerical models.

Acknowledgements. We would like to thank the Central Weather Bureau, Taiwan, for providing the data. This work was supported by NSC-2111-M-001-004-MY3.

ACPD

10, 13495–13517, 2010

References

Brand, S. and Blelloch, J. W.: Changes in the characteristics of typhoons crossing the island of Taiwan, Mon. Weather Rev., 102, 708–713, 1974.

Chien F. C., Liu, Y. C., and Lee, C. S.: Heavy rainfall and southwesterly flow after the leaving of typhoon Midulle (2004) from Taiwan., J. Meteorol. Soc. Japan, 86, 17–41, 2008.

Chen, Y.-L. and Li, J.: Characterisitics of surface air flow and pressure patterns over the island of Taiwan during TAMEX, Mon. Weather Rev., 123, 695–716,1995,.

Ge, X., Li, T., Zhang, S., and Peng, M.: What causes the extremely heavy rainfall in Taiwan during Typhoon Morakot (2009)?, Atmos. Sci. Lett., 11, 46–50, 2010.

Knutson, T. R., Sirutis, J. J., Garner, S. T., Held, I., and Tuleya, R. E.: Simulation of the recent multidecadal increase of Atlantic hurricane activity using an 18-km-grid regional model, B. Am. Meteorol. Soc., 88, 1549–1565, 2007.

Lee, C. S., Liu, Y.-C., and Chien, F. C: The secondary low and heavy rainfall associated with Typhoon Mindulle (2004), Mon. Weather Rev., 136, 1260–1283.,2008.

Lin C.-Y and Chen, C. S.: A study of orographic effects on mountain-generated precipitation systems under weak synoptic forcing, Meteorol. Atmos. Phys., 81, 1–25, 2002.

Lin, Y.-L., Chiao, S., Wang, T. A., Kaplan, M. L., and Weglarz, R. P.: Some common ingredients for heavy orographic rainfall, Weather Forecast., 16, 633–660, 2001.

Lin, Y. L, Ensley, D. B., Chiao, S., and Huang, C. Y.: Orographic influences on rainfall and track deflection associated with the passage of a tropical cyclone, Mon. Weather Rev., 130, 2929–2950, 2002.

Skamarock, W. C., Klemp, J. B., Dudhia, J., Gill, D. O., Barker, D. M., Duda, M., Huang, X.-Y., Wang, W., and Powers, J. G.: A Description of the Advanced Research WRF Version 3, NCAR Technical Note, 2008.

Wu, C. C. and Kurhara, Y.: A numerical study of the feedback mechanisms of hurricane-environment interaction on hurricane movement from the potential vorticity perspective, J. Atmos. Sci., 53, 2264–2282, 1996.

Wu, C. C. and Kuo, Y.-H.: Typhoons affecting Taiwan: Current understanding and future challenges, B. Am. Meteorol. Soc., 80, 67–80, 1999.

Wu, C. C., Yen, T. H., Kuo, Y. H., and Wang, W.: Rainfall simulation Associated with Typhoon Herb(1996) near Taiwan. Part I: The topographic effect, Weather Forecast., 17, 1001–1015, 2002.

Yang, M. J., Zhang, D. L., and Huang ,H. L.: A modeling study of Typhoon Nari (2001) at landfall Part I: Topographic effects, J. Atmos. Sci., 65, 3095–3115, 2008.

ACPD

10, 13495–13517, 2010

Table 1. Record of the 10 highest typhoon accumulation rainfalls during the last 50 years. Stations' elevation for A-Li station, An Pu and Chu Tze Hu are 2413 m, 826 m and 607 m, respectively. (TC: Tropical Cyclone, NE: Northeasterly, SW: southwesterly).

Typhoon name (CWB warning period)	Intensity classification* Characteristics	Accumulation rainfall in mm (duration) station	Casualties including Death and missing
MORAKOT 2009/08/5–10	Intermediate TC Traversing CMR+ SW monsoon	2855 mm (100 h) A-Li Shan	695
FLOSSIE 1969/10/1–7	Intermediate TC nearby + NE monsoon	2162 mm (120 h) An Pu	105
HERB 1996 07/29–08/01	Strong TC Traversing CMR	1987 mm (48 h) A-Li Shan	73
LYNN 1987/10/23–27	Strong TC nearby + NE monsoon	1497 mm (96 h) Chu Tze Hu	63
SINLAKU 2008/09/9–17	Strong TC Traversing CMR	1458 mm (96 h) A-Li Shan	21
ORA 1978/10/11–14	Intermediate TC nearby + NE monsoon	1434 mm (96 h) Chu Tze Hu	7
GLORIA 1963/9/8–13	Strong TC nearby + NE monsoon	1433 mm (96 h) A-Li Shan	363
NARI 2001/9/6–20	Intermediate TC Traversing CMR	1304 mm (72 h) Chu Tze Hu	104
HAITANG 2005/7/16–20	Strong TC Traversing CMR	1216 mm (72 h) A-Li Shan	15
MINDULLE 2004/06/28–07/02	Intermediate TC Traversing CMR	1182 mm (72 h) A-Li Shan	45

* The CWB's classification of typhoons is based on the maximum wind speed: the light typhoon: 17.2–32.6 m/s; the intermediate typhoon: 32.7–50.9 m/s; the severe typhoon: ≥51 m/s.

Discussion Paper | Discussion Paper | Discussion Paper | Discussion Paper |

ACPD

10, 13495–13517, 2010

Mesoscale processes for super heavy rainfall of Typhoon Morakot

C.-Y. Lin et al.

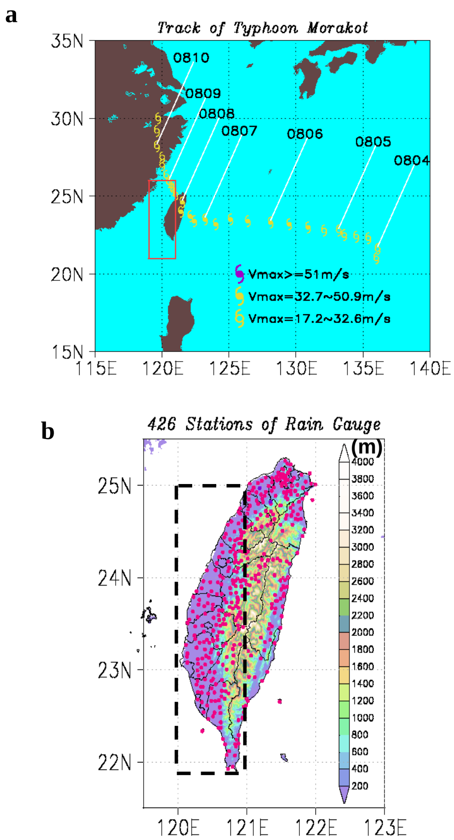

Fig. 1. (a) The best tracks for Typhoon Morakot (2009). Colored solid (open) typhoon symbol indicates the best track and the intensity of typhoon in 6 h interval. **(b)** Spatial distribution of the rainfall stations monitoring network (red dots) and topographic high (colored) over Taiwan. The black dashed square is the rainfall convert area calculated in Fig. 1c.

ACPD
10, 13495–13517, 2010

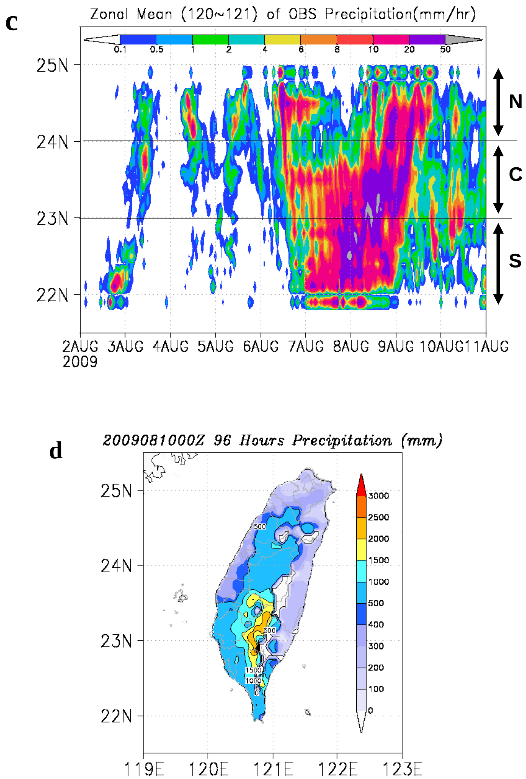

Fig. 1. **(c)** Spatial and temporal variation of the average rainfall on the 0.1° latitude interval between 120 and 121° E over western Taiwan. **(d)** 96-h accumulation rainfall amount from 00 00UTC 6 to 00:00 UTC 10 August 2009.

ACPD
10, 13495–13517, 2010

e

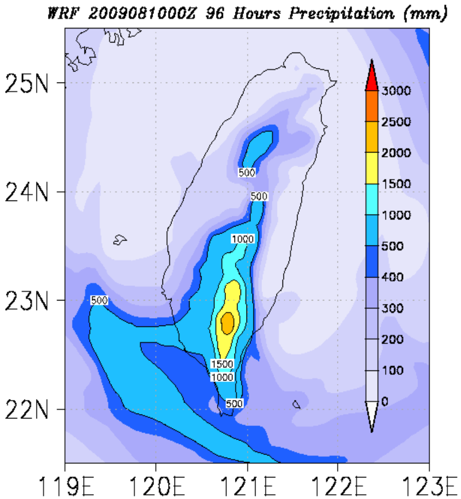

Fig. 1. (e) Result of simulation accumulation rainfall amount during 00:00 UTC 6 to 00:00 UTC 10 August 2009 by WRF model.

ACPD
10, 13495–13517, 2010

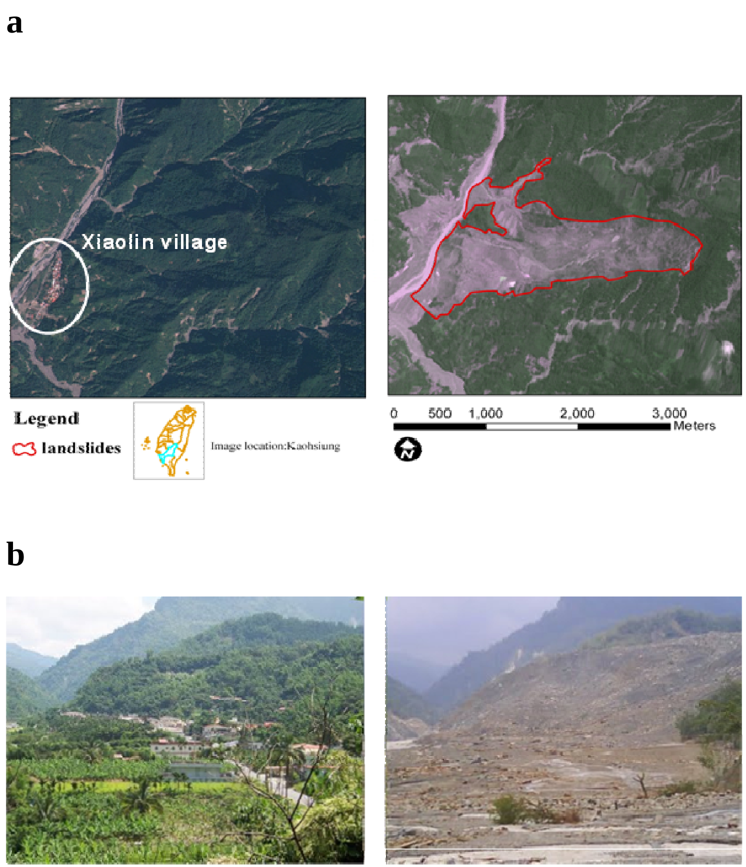

Fig. 2. **(a)** Image before (left) and after (right) the landslide around Xiaolin village over southern Taiwan from FORMASAT-2 satellite. **(b)** Photo taken at the Xiaolin village before (left) and after (right) the landslide (source: http://www.wretch.cc/album/show.php?i=Magicsky\&b=32764\&f=1989748477\&p=102).

ACPD
10, 13495–13517, 2010

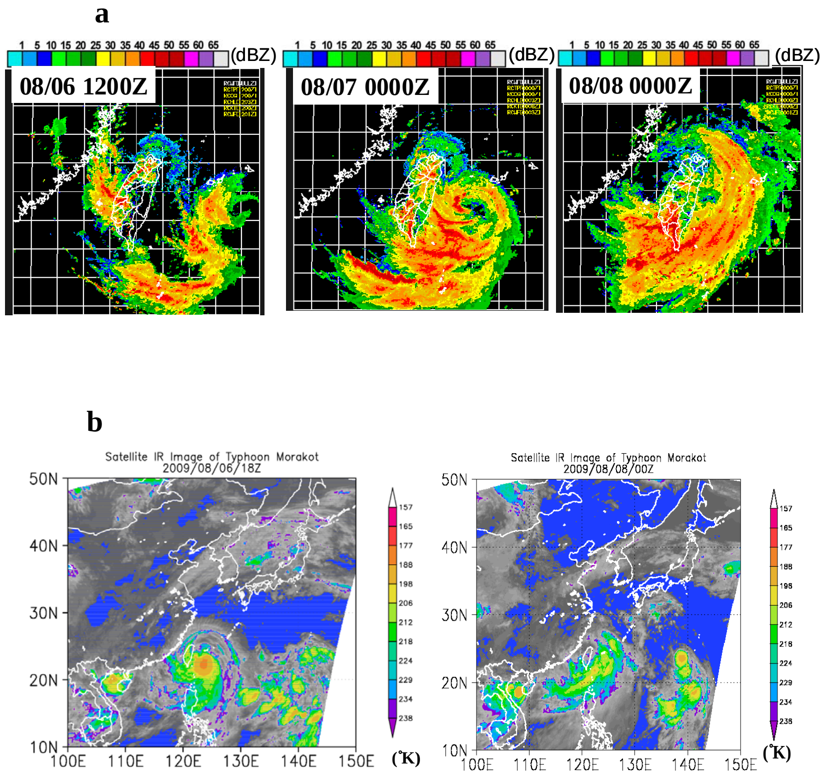

Fig. 3. **(a)** Composite of vertical maximum radar reflectivity (colored) at 12:00 UTC 6, 00:00 UTC 7 and 00:00 UTC 8 August, 2009. **(b)** Infrared Satellite image from Japan MTSAT satellite at 18:00 UTC 6 and 00:00 UTC 8 August, 2009. The colored areas represent for the temperature scale (˚K).

ACPD
10, 13495–13517, 2010

Mesoscale processes for super heavy rainfall of Typhoon Morakot

C.-Y. Lin et al.

Title Page
Abstract
Introduction
Conclusions
References
Tables
Figures
◀︎
▶︎
Back
Close
Full Screen / Esc
Printer-friendly Version
Interactive Discussion

ACPD
10, 13495–13517, 2010

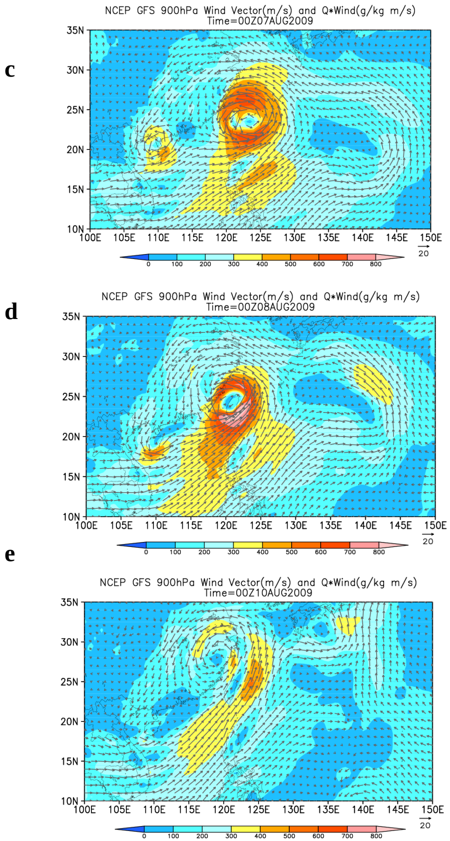

Fig. 3. **(c)** Moisture flux (colored) and wind field (arrow) deduced from NCEP GFS data sets at 900 hPa level at 00:00 UTC 7 August, 2009. The colored scales represent the magnitude of moisture flux. The lower right corner of arrow denotes the scale of wind speed. **(d)** Same as **(c)** but for 00:00 UTC 8 August, 2009. **(e)** Same as **(c)** but for 00:00 UTC 10 August, 2009.

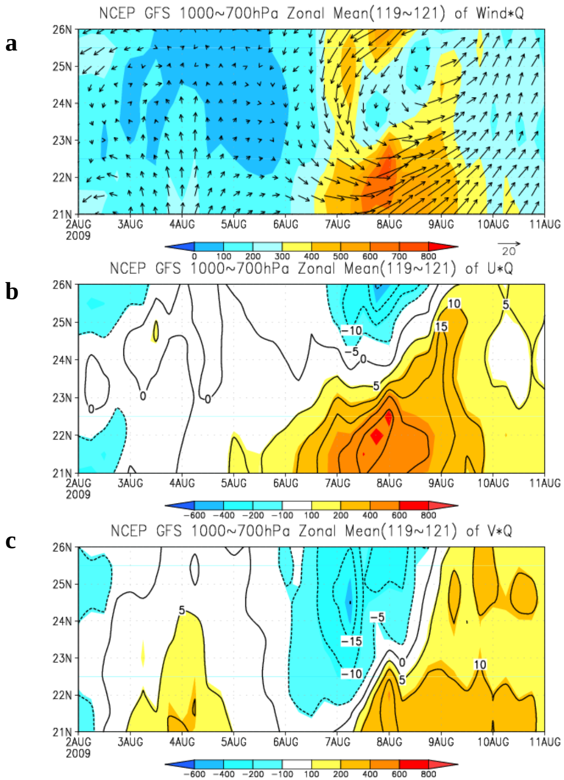

Fig. 4. **(a)** Temporal variation of average moisture flux (colored) and wind field (arrow) for the zonal mean (119–121° E) and depth between 1000 and 700 hPa deduced from NCEP GFS data sets. The colored scales represent the magnitude of moisture flux. The lower right corner of arrow denotes the scale of wind speed. **(b)** Temporal variation of the average moisture flux (colored) and wind speed (contour) between 1000 and 700 hPa for the zonal mean (119–121° E) in E-W direction deduced from NCEP GFS data sets. The colored scales represent the magnitude of moisture flux. The lower right corner of arrow denotes the scale of wind speed. **(c)** Temporal variation of the average moisture flux (colored) and wind speed (contour) between 1000 and 700 hPa for the zonal mean (119–121° E) in N-S direction deduced from NCEP GFS data sets. The colored scales represent the magnitude of moisture flux. The lower right corner of arrow denotes the scale of wind speed.

ACPD

10, 13495–13517, 2010

Mesoscale processes for super heavy rainfall of Typhoon Morakot

C.-Y. Lin et al.

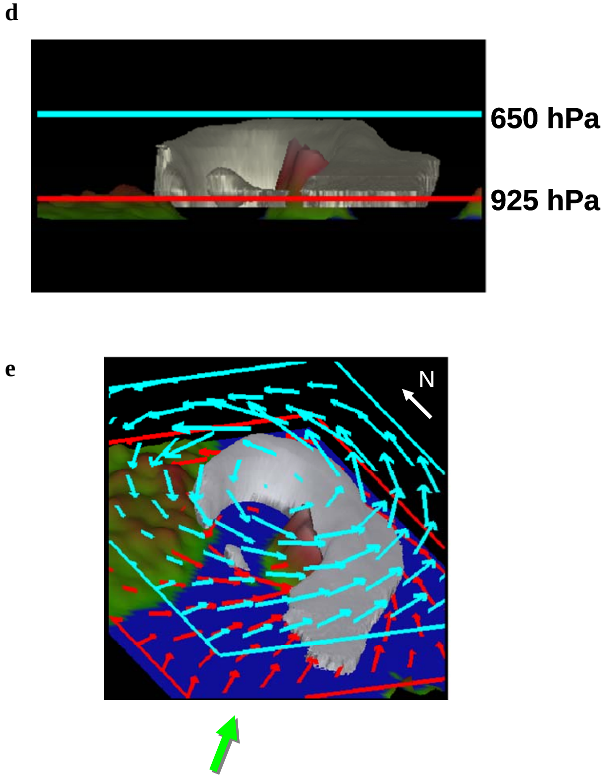

Fig. 4. (d) A northwest-southeast vertical perspective views for depth by VIS5D for the moisture flux at 00:00 UTC 8 August taken from the direction of the arrow in Fig. 4e. The grey shading is the moisture flux surface of 550 g/kg m/s. **(e)** Three-dimensional perspective views by VIS5D for the moisture flux at 00:00 UTC 8 August. The blue (red) arrow is the wind field at 650 hPa (925 hPa). The grey shading is the moisture flux surface of 550 g/kg m/s.

ACPD
10, 13495–13517, 2010

Mesoscale processes for super heavy rainfall of Typhoon Morakot

C.-Y. Lin et al.

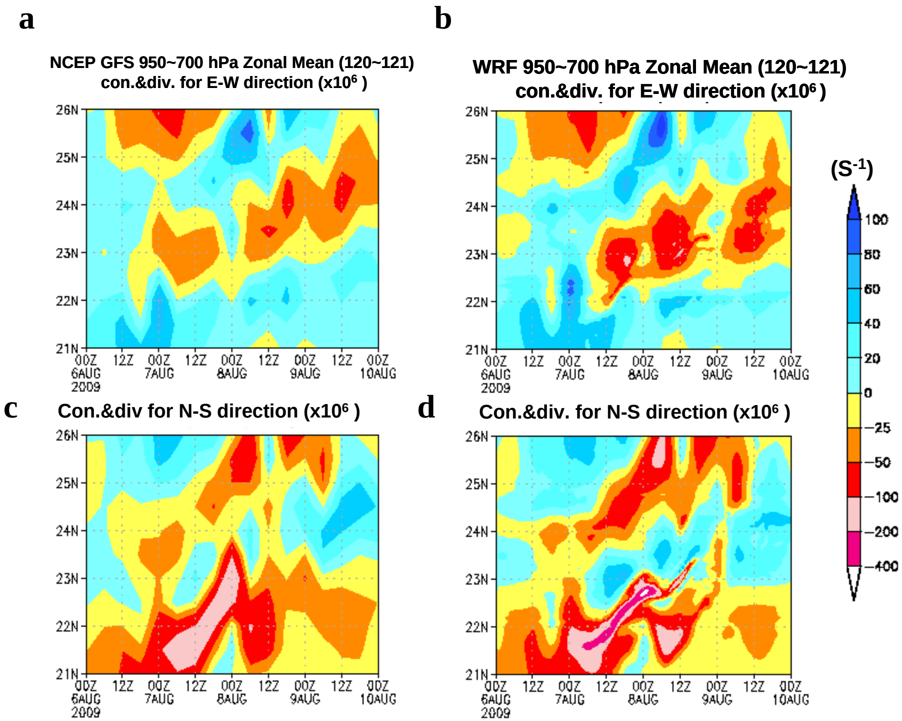

Fig. 5. **(a)** Temporal variation of wind convergence (negative) and divergence (positive) in E-W direction (colored) between 950 and 700 hPa for the zonal mean (119–121° E) deduced from NCEP GFS data sets. **(b)** Temporal variation of wind convergence (negative) and divergence (positive) in N-S direction (colored) between 950 and 700 hPa for the zonal mean (119–121° E) deduced from NCEP GFS data sets. **(c)** Simulated results of the temporal variation of wind convergence (negative) and divergence (positive) in E-W direction (colored) between 950 and 700 hPa for the zonal mean (119–121° E) from WRF model. **(d)** Simulated results of the temporal variation of wind convergence (negative) and divergence (positive) in N-S direction (colored) between 950 and 700 hPa for the zonal mean (119–121° E) from WRF model.

ACPD
10, 13495–13517, 2010